surgeon checks the presence of metastasis in the lymph nodes after the removal of the tumor. In the second case, the gamma locator can detect tumors located superficially, and accurately determine their boundaries [2].
When selecting the scintillator the following requirements should be considered: high relative light yield compared to NaI(Tl), the high value of the effective atomic number. The lanthanum cerium bromine has demonstrated the best features: the light yield higher than that of NaI(Tl) (130%), high density, high atomic number provide high efficiency of photoelectric absorption of gamma rays, and the decay time of the order of tens of nanoseconds provides high temporal resolution of the detector. Silicon photomultiplier is a device for detection of low intensive and very fast (several hundred nanosecond duration) light flashes. SiPM is used due to its high detection efficiency, low bias voltage, compact dimensions and high gain of signals. Experimental studies have shown that a scintillator packaged together with the photodetector provides 4,1% FWHM energy resolution at 662 keV (Cs-137).
Gamma locator is constructed in cordless configuration and equipped with a lithium-ion battery. Indication is performed by an acoustic signal and LED. Adjusting of the bias voltage of the photodetector and the thresholds of the discriminator is carried out by changing the resistance of the trimmers.
The main technical characteristics of the prototype gamma locator were determined in the laboratory of NRNU MEPhI according to the NEMA NU3-2004 protocol [3]. Spatial resolution of gamma locator is the minimum distance between two point sources on which they can be resolved separately, or FWHM of the dependence of counting rate of the transverse distance between the detector and the source, and is measured to be 20 mm. Spatial selectivity is the polar angle, at which the count rate drops twice and it is measured to be 26 degrees. Sensitivity is 118 cps/MBq.
For the comparison performance of scintillation and semiconductor gamma locator the NEMA testing of the semiconductor CdTe-based commercial gamma probe was performed. The field of view of the CdTe gamma probe was formed with a lead collimator with 3 mm diameter aperture. Spatial resolution was measured to be 22 mm, and angular resolution is 30 degrees.

Keywords: gamma probe, miniature gamma detector, radioguided surgery

References:
[1] A. K. Yagnyukova, A. I. Bolozdynya, V. A. Kantserov, et al, "A γ Probe for Radionuclide Diagnostics of Cancer", Instruments and Experimental Techniques, 2015, Vol. 58, No. 1, pp. 153–157
[2] P. Fougeres, A. Kazandjian, V. Prat, H. Simon, M. Ricard, J. Bede, "Sentinel node in cancer diagnosis with surgical probes", Nucl. Instrum. and Methods in Physics Research. 2001. V. A 458. P. 34.
[3] Performance measurements and quality control guidelines for non-imaging intraoperative gamma probes, NEMA Standards Publication NU 3-2004.

21

Evaluation of the size of micrometric/nanometric dosimeters for use in radiotherapy and medical physics

M. Cunha[1], E. Testa[1], M. Beuve[1], J. Balosso[2,3], A. Chaikh[2,3]
[1] Université de Lyon, F-69622, Lyon, France; Université de Lyon 1, Villeurbanne; CNRS/IN2P3, Institut de Physique Nucléaire de Lyon
[2] Department of Radiation Oncology and Medical Physics, Grenoble University Hospital.
[3] Univ. Grenoble-Alpes, Grenoble, France.

When treating tumors with radiotherapy, it is of utmost importance to ensure that the prescribed dose is accurately delivered to the target volumes. In that sense, *in-vivo* dosimetry in real time was recently implemented in radiotherapy departments. Dosimeter performance depends necessarily on physical and geometrical parameters (e.g. beam energy and distance from source to skin), which implies the use of correction factors. Implantable dosimeters are therefore preferable in order to minimize the need for corrections. They should be as small as possible, but still they should provide reliable measurements to comply with the requirements of clinical practice in routine radiotherapy. The state-of-the-art of these kind of dosimeters was the subject of a review elsewhere (1), which reported that implantable detectors of submillimetric size are currently available. The purpose of this study is to assess by Monte-Carlo simulations how much the size of such dosimeters can be decreased without jeopardizing their performance in a clinical environment.
First, the interaction of photons from a ^{60}Co source with water was simulated with a Monte-Carlo tool (2). The calculations were performed for 0.3, 0.1, 1, 3 and 10 Gy. Then, the distributions of specific energy were obtained for volumes representing dosimeters at nanometric and micrometric scales. Cylinders with equal radii of 0.3, 0.1, 1, 3 and 10 µm were used for this purpose. The mean specific energy $\langle z_t \rangle$ was calculated for each case. To evaluate how the dosimeter size would impact its performance in a clinical scenario, the probability *p* that a dosimeter measurement falls outside a given interval defined around $\langle z_t \rangle$ was estimated. Intervals were defined as $[\langle z_t \rangle - \gamma \langle z_t \rangle ; \langle z_t \rangle + \gamma \langle z_t \rangle]$ with γ equal to 3%, 5% and 10%.
The pattern of the distributions of specific energy evolves with dosimeter size and irradiation dose. Fixing the irradiation dose and decreasing the dosimeter radius or fixing the radius and decreasing the irradiation dose strongly widened the range in measured values of specific energy, but also increased the probability of yielding a non-null measurement. In turn, for higher doses and radii, distributions tend to Gaussian curves.

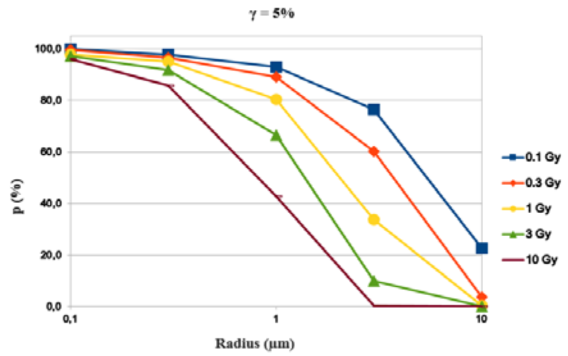

Concerning the probability of obtaining a measurement outside the defined interval, the larger the interval, the irradiation dose, and the dosimeter radius, the smaller this probability became (see figure above).
The simulation results showed that dosimeters at a nanometric scale are not able to yield statistically-reproducible measurements and are therefore unfit for use in clinical practice. Increasing the size to micrometric scale led to a decrease in the statistical fluctuations. Nevertheless, to have enough accuracy at routine clinical doses (approximately 2 Gy in the tumor volume), a dosimeter radius of at least 10 µm is required.

Keywords: radiotherapy; nano/microdosimeter; Monte-Carlo simulations

References
[1] Chaikh A, Beuve M, Balosso J. Nanotechnology in radiation oncology: The need for implantable nano dosimeters for in-vivo real time measurements. Int J Cancer Ther Oncol [Internet]. 2015 [cited 2015 Oct 30];3(2). Available from: http://www.ijcto.org/index.php/IJCTO/article/view/ijcto.3 2.17
[2] Gervais B, Beuve M, Olivera GH, Galassi ME. Numerical simulation of multiple ionization and high LET effects in liquid water radiolysis. Radiat Phys Chem. 2006 Apr;75(4):493–513.

22

From 2D to 3D: Proton radiography and proton CT in proton therapy: A simulation study

J. Takatsu[1], E. R. van der Graaf[2], M-J. van Goethem[3], S. Brandenburg[2],
A. K. Biegun[2]
[1] Department of Radiation Oncology, Graduate School of Medicine, Osaka University, Japan
[2] KVI-Center for Advanced Radiation Technology, University of Groningen, The Netherlands
[3] Department of Radiation Oncology, University Medical Center Groningen, University of Groningen, The Netherlands

Purpose: In order to reduce the uncertainty in translation of the X-ray Computed Tomography (CT) image into a map of proton stopping powers (3-4% and even up to 10% in regions containing bones [1-8]), proton radiography is being studied as an alternative imaging technique in proton therapy. We performed Geant4 Monte Carlo simulations for a 2-dimentional (2D) proton radiography system to obtain directly proton stopping powers of the imaged object. In the next step, the object was rotated every 10 degrees to obtain the 3D proton CT, and the iterative reconstruction method was used to reproduce the image.
Materials/methods: In our proton radiography simulation setup (figure) we used two ideal (100% efficiency) position sensitive detectors (red squares), with the size of 10x10 cm^2 each, to track a single proton entering and exiting a phantom under study. The residual energy of a proton was detected by a BaF_2 crystal (yellow cylinder), with a diameter of 15 cm, placed after the second position sensitive detector. A cylindrical phantom with a 2.5 cm diameter and 2.5 cm height was made of CT solid water (Gammex 357, ρ=1.015 g/cm^2) and filled with different materials: PMMA (ρ=1.18 g/cm^2, red insert), air (ρ=1.21•10^{-3} g/cm^2, below and/or above each inserts), and tissue-like materials: adipose (Gammex 453, ρ=0.92 g/cm^2, yellow insert) and cortical bone (Gammex 450, ρ=1.82 g/cm^2, blue insert) [9]. The phantom was irradiated with 3x3 cm^2 scattered proton beam with an energy of 150 MeV. It was irradiated with 2•10^5 protons at each of the 36 rotation angles. The phantom was placed perpendicularly to the beam direction allowing a proton to pass through a number of materials with different densities.

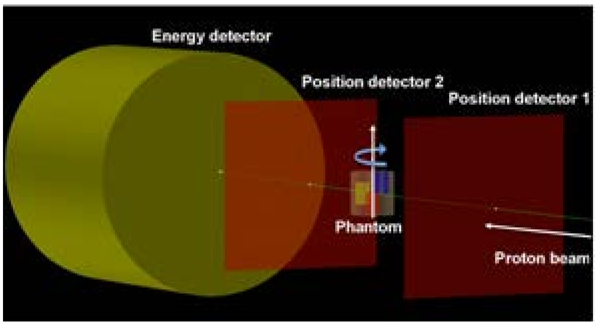

Results: First, the energy loss radiographs (a difference between proton beam energy and residual energy deposited in the energy detector) at each of the 36 phantom rotation angles were created. For the iterative reconstruction algorithm, a reference image of the phantom was created in two ways: (1) based on the energy loss in different phantom materials simulated with Geant4, and (2) using a simple back projection algorithm. The reconstruction agrees well with the actual phantom. A maximum of 50 iterations were used showing the smallest mean squared error already after 5 iterations.
Conclusion: First attempt to iteratively reconstruct the cylindrical phantom with more materials on the proton beam shows a satisfactory result. To improve the reconstruction at the material boundaries, additional local iterations will be applied.

Keywords: Proton radiography, proton CT, treatment planning

References:
[1] U. Schneider and E. Pedroni, *Proton radiography as a tool for quality control in proton therapy*, Med Phys 22(4) (1995) 353-363
[2] U. Schneider, E. Pedroni and A. Lomax, *The calibration of CT Hounsfield units for radiotherapy treatment planning*, Phys Med Biol 41 (1996) 111-124
[3] W. Schneider, T. Bortfeld and W. Schlegel, *Correlation between CT numbers and tissue parameters needed for Monte Carlo simulations of clinical dose distributions*, Phys Med Biol 45 (2000) 459-478
[4] G. Cirrone et al., *The Italian project for a proton imaging device*, Nucl Instr Meth in Phys Res A576 (2007) 194-197
[5] H. Paganetti, *Range uncertainties in proton therapy and the role of Monte Carlo simulations*, Phys Med Biol 57 (2012) R99-R117
[6] T. Plautz et al., *200 MeV Proton Radiography Studies with a Hand Phantom Using a Prototype Proton CT Scanner*, IEEE Trans on Med Imag 33 (4) (2014) 875-881
[7] G. Landry et al., *Deriving concentrations of oxygen and carbon in human tissues using single- and dual-energy CT for ion therapy applications*, Phys Med Biol 58 (2013) 5029–5048
[8] J. Schuemann et al., *Site-specific range uncertainties caused by dose calculation algorithms for proton therapy*, Phys Med Biol 59 (2014) 4007-4031
[9] www.gammex.com

23
GPU based iterative CBCT for prospective motion compensated algorithm for radiation therapy
Author names – Initial. Surname (order the authors as you would like them to appear; underline the speaker's name)
A. Biguri[1], M. Dosanjh[2], S. Hancock[2], M. Soleimani[1]
[1] Engineering Tomography Lab (ETL), Electronic and Electrical Engineering, University of Bath, UK
[2] CERN, Geneva, Switzerland

Purpose: One of the common imaging techniques in image guided radiation therapy (IGRT) is cone beam computed tomography (CBCT). CBCT is used for tumor localization in pre-treatment planning. In lung radiation therapy, the motion artefacts severely affect the quality of reconstructed images. As the data acquisition can take over a minute, the motion generated by the patient breathing can distort the tomograms, this distortion being propagated in the image reconstruction step. We propose an electrical impedance tomography (EIT)-CBCT dual modality for motion corrected image reconstruction [2]. Iterative algebraic reconstruction method can potentially provide a suitable image reconstruction tool for such dual modality. This paper present an improved GPU based CBCT image reconstruction. Efficient computation of forward and backward projections is implemented in GPU, which is the main building block of various iterative reconstruction methods.
Materials/methods: The projection and backprojection steps have been accelerated in our GPU code, using the Compute Unified Device Architecture (CUDA) [1]. The ray-driven projection uses the texture memory that has a hardware implemented trilinear interpolation. Using a per-ray separation for the multithreading step, the integral of the x-rays is computed, with a user specified length that defines the tradeoff between for accuracy and speed. In the backprojection step, a voxel-based weighted backprojection is performed, similar to the Feldkamp Davis Kress (FDK) algorithm, to avoid the aliasing effect common in algebraic methods with diverging rays [4]. To simulate reality a human thorax-like digital phantom has been used. Limited (45) projections have been simulated and Poisson noise added. The commonly use FDK and simultaneous iterative reconstruction technique (SART) have been simulated.
Results: Figure 1 shows the reconstructed images. For a 512^3 voxels with 512^2 detector pixels the GPU based code takes 5s for FDK and a single SART iteration on the high precision setting (integral length= voxel size/10), and 0.5s for a similar precision as a matrix based method (integral length= voxel size). The image reconstructed with SART had 300 iterations, 2.5 minutes in the lower precision setting.